JMEPEG (2011) 20:997–1002
DOI: 10.1007/s11665-010-9714-1

1059-9495/$19.00

Influence of Isothermal Bainite Transformation Time on Microstructure and Mechanical Properties of Hot-Dip Galvanized TRIP Steel

Wei Ding, Di Tang, Haitao Jiang, and Wei Huang

(Submitted August 27, 2009; in revised form May 2, 2010)

The influence of isothermal bainitic transformation (IBT) time on microstructure and mechanical properties of hot-dip galvanized TRIP steel with 0.20C-1.50Mn-1.2Al-0.26Si was investigated using optical microscopy, x-ray diffraction (XRD), Transmission Electron Microscope (TEM), dilatometry, and mechanical testing. This steel has high tensile strength of over 780 MPa with elongation more than 22%. The microstructure of the steel mainly consisted of ferrite, bainite, retained austenite, and martensite. The metastable austenite remaining after bainitic transformation will be transformed into martensite at the final cooling stage. The IBT time affects retained austenite content. When the IBT increased from 10 to 60 s, the amount of retained austenite increased from 9.40 to 15.42%, correspondingly. The IBT time also affects the strain hardening behavior. The *n* value characteristics of samples for IBT time from 10 to 30 s are similar to those of DP steel; however, the *n* value of specimen with IBT of 60 s shows features typical of TRIP steel.

Keywords hot-dip galvanized TRIP steel, mechanical properties, *n* value, retained austenite

1. Introduction

The TRIP steels show high strength values in combination with an excellent deformability (Ref 1, 2). These mechanical properties are brought about by the TRIP steel microstructure which consists of ferrite, bainite, sometimes a small amount of martensite, and retained austenite which transforms to martensite during deformation (Ref 3). This multiphase microstructure is usually generated by a standard two-stage heat treatment (Ref 4). The first stage consists in an intercritical annealing (IA) during which controlled volume fractions of austenite and ferrite are formed. This IA is then followed by an isothermal stage in the bainite transformation temperature range. During this second stage, partial transformation of the austenite to bainite leads to the stabilization of the remaining austenite at room temperature (Ref 5). Isothermal bainitic transformation (IBT) time and temperature of the second stage have a decisive influence on the mechanical properties of TRIP steel (Ref 6).

Apart from the ever increasing demand for a higher standard in respect of environmental friendliness, car materials are required to be more durable. Therefore, the technique of using hot-dip galvanized steel sheet is the perfect choice for car manufacturing (Ref 7). Due to the speciality of hot-dip galvanizing technique (Ref 8, 9) (with Si content less than 0.3%, short IBT time, etc.), the traditional TRIP steel content design and manufacturing technique can no longer fulfill the requirement for hot-dip galvanizing. As a result, hot-dip galvanized TRIP steel was worthy to study.

A TRIP steel that can be used with hot-dip galvanizing was investigated in this study. The phase transformation behavior of the steel was investigated. In particular, the influence of IBT on microstructure and mechanical properties (yield strength, tensile strength, elongation, strength-ductility balance, stress-strain curve, and strain hardening behavior) of the steel was investigated in this study.

Wei Ding, Di Tang, Haitao Jiang, and **Wei Huang**, National Engineering Research Center for Advanced Rolling Technology, University of Science & Technology, Beijing, Beijing 100083, China. Contact e-mail: adingwei@126.com.

2. Experimental Procedure

The chemical composition of the TRIP steels used in this study is given in Table 1. The hot-dip galvanized TRIP-aided steel was prepared as 50 kg ingot in an air induction furnace. The cast ingot was forged into a 1000 mm × 70 mm × 60 mm block. Small blocks of 120 mm × 70 mm × 60 mm were cut from forged stock. These 60-mm thick blocks were soaked at 1200 °C for 1.5 h, and hot rolled to a thickness of 4.2 mm in six passes. The hot-rolled plates were pickled in a 25 vol.% HCl solution and subsequently cold rolled to achieve a final thickness of 1.4 mm.

The phase transformation behavior was studied by means of dilatometry. Solid cylindrical samples with a diameter of 4 mm and a length of 10 mm, cut from hot-rolled sheet, with an initial pearlite-ferrite microstructure, were heated to 1100 °C at 10 °C s^{-1} under vacuum. A dialatometer was used to measure dilatation across the length change of the sample. A_{c1} and A_{c3} temperatures were determined by dilatatometry curves.

In order to obtain TRIP-aided steel, a two-step heat treatment was used. The samples were heat treated in Gleeble3500. Four different heat treatment regimes with different IBT time were designed, the detail are summarized

in Table 2. Heat-treated samples were prepared for microstructural study with 10% $Na_2S_2O_5$ color-etching technique (Ref 10). The volume fraction of retained austenite and its carbon content after the heat treatment were measured using XRD. TEM analysis was performed using a JEOL 2010 TEM. The acceleration voltage was 200 kV.

The room temperature tensile properties of the heat-treated samples were examined on a gauge length of 50 mm with a 12.5-mm nominal width. Tensile tests were carried out in a SANS universal testing machine using a load range of 5000 kgf. The crosshead speed was maintained at 3 mm/min.

3. Results and Discussion

3.1 Phase Transformation Behavior

Solid cylindrical samples were heated to 1100 °C at a rate of 10 °C s^{-1} to determine A_{c1} and A_{c3} which were found to be 750 and 980 °C, respectively, as illustrated in Fig. 1(a). Compared with the traditional high-Si TRIP steel, the two-phase region of hot-dip galvanized TRIP steel with low-Si and high Al is very wide, which shows that adding Al can significantly expand the two-phase region, especially for A_{c3}.

The thermal dilatation was measured for both the ferrite and the austenite, and the transformed fraction was calculated from the dilatation curve. The resulting transformed fraction is shown in Fig. 1(b).

3.2 Microstructure Characterization

Figure 2 shows the microstructure of the steel before cold rolling and heat treatment. It shows a pearlite-ferrite microstructure.

Figure 3 shows optical microstructure of the samples A (t_{IBT} = 10 s) and C (t_{IBT} = 30 s) after cold rolling and heat treatment. Various phases in the microstructure are identified in Fig. 3: the areas displayed as off-white are ferrite, the bright white ones are retained austenite, brown regions are bainite, and dark ones are martensite. It can be seen that the content of austenite in sample C (t_{IBT} = 30 s) is much more, compared with sample A (t_{IBT} = 10 s). Retained austenite phase is homogeneously distributed throughout the microstructure, and is connected to adjacent ferrites or bainites.

Figure 4 shows TEM micrographs of the heat-treated sample C. It shows isolated acicular retained austenite particles in ferrite matrix (the bright field, Fig. 4a). Figure 4(b) shows the dark field, and Fig. 4(c) shows the selective area diffraction pattern. This clearly confirms the presence of the retained austenite. From Fig. 3 and 4(a), it can be found that there are two kinds of retained austenite in the hot-dip galvanized TRIP steel. The first one can be classified as a block structure along the ferrite grain boundary which is clearly shown in Fig. 3. The second is an acicular structure seen in ferrite matrix as shown

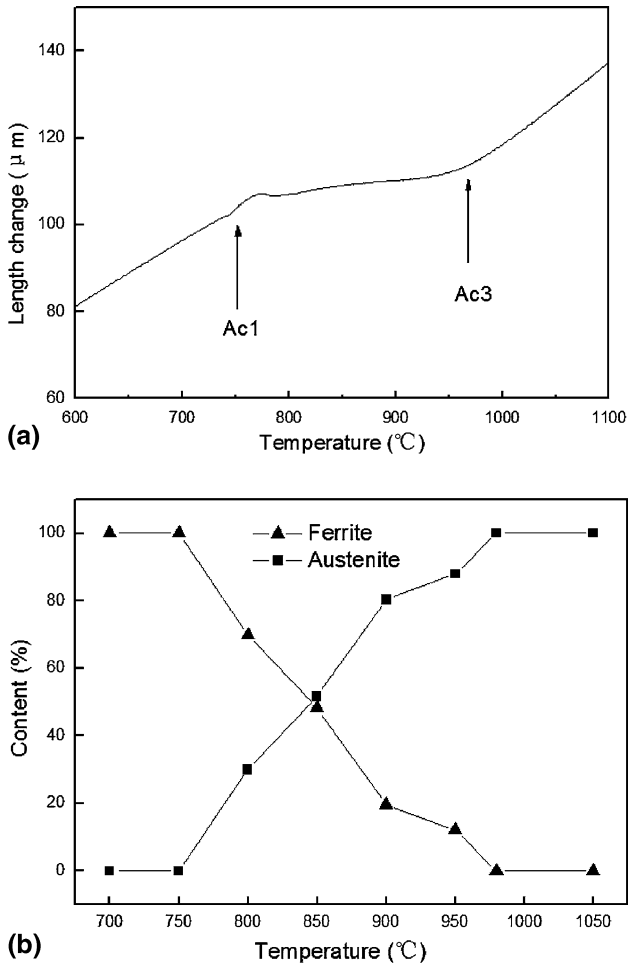

Fig. 1 (a) Dilatation vs. temperature for determination of A_{c1} and A_{c3} (heating rate 10 °C s^{-1}) of investigated steel and (b) Transformation content vs. transformation temperatures of investigated steel

Table 1 Chemical composition (wt.%) of investigated steel

Element	C	Mn	Si	Al	S	P	N	Nb + V
Content/%	0.20	1.50	0.26	1.28	0.005	0.007	<0.006	0.13

Table 2 Heat-treatment regimes of the investigated steel

Samples	Heating rate, °C s^{-1}	IA temperature, °C	IA time, s	Rapid cooling rate, °C s^{-1}	IBT temperature, °C	IBT time, s	Final cooling rate, °C s^{-1}
A	10	850	60	−20	460	10	−20
B	10	850	60	−20	460	20	−20
C	10	850	60	−20	460	30	−20
D	10	850	60	−20	460	60	−20

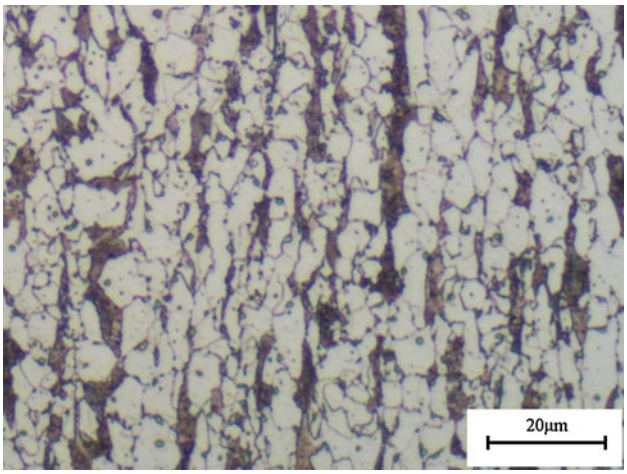

Fig. 2 Microstructure of investigated steel after hot-rolled (etchant: 4% nital)

in Fig. 4(a). The morphology of the retained austenite as shown in Fig. 3 and 4(a) is in accordance with the conventional TRIP steel (Ref 11).

From Fig. 4(d)-(f), it is clear that martensite (the illuminated phases in the dark field condition) is in ferrite matrix. Martensite is expected to be formed by transformation of austenite with low carbon content after IBT. The too short IBT time, as the inherent characteristics of hot-dip galvanized TRIP steel, is the reason why martensite in the hot-dip galvanized TRIP steel is inevitable. Therefore, the microstructure of the hot-dip galvanized TRIP steel consists of ferrite, bainite, retained austenite, and martensite.

The volume fraction of retained austenite in the heat-treated samples was determined by x-ray diffraction (XRD) using Cu Kα radiation. The integrated intensities of the (200) and (211) peaks of ferrite, and the (200), (220), and (311) peaks of austenite were used for this purpose, and the volume fraction of the retained austenite was calculated.

For the calculation of the carbon content of the retained austenite (Cγ), the lattice parameter a_0 was measured from the fcc(220) diffraction peak using the Eq 1.

$$C\gamma = (a_0 - 3.571)/0.044 \quad \text{(Eq 1)}$$

Figure 5 shows the measured XRD data for the heat-treated samples. The results are shown in Table 3. It can be seen that as the IBT time is increased from 10 to 60 s, the amount of the retained austenite increased from 9.40% (sample code A) to 15.42% (sample code C). The reason is that short IBT time leads to the birth of thermally unstable austenite which transforms to martensite during final cooling after the bainite transformation treatment. Furthermore, the carbon content of the retained austenite increased with the increase in the IBT time. This is caused by the enrichment of carbon in austenite during the bainite transformation.

3.3 Mechanical Properties

Tensile specimens from the rolling direction were tested. The results (yield strength (YS), tensile strength (TS), elongation (EL), and the strength-ductility balance (TS × EL)) are summarized in Table 4. Except for the sample A, the rest of

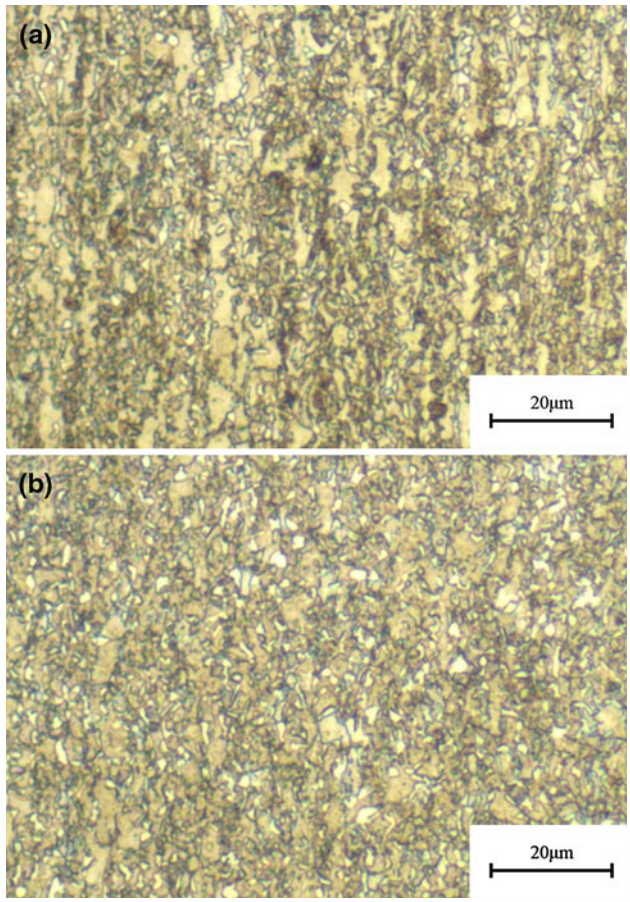

Fig. 3 Microstructure of investigated steel after cold rolling and heat treatment: (a) sample A and (b) sample C, etchant: 10% $Na_2S_2O_5$ (Martensite dark, Ferrite off-white, Austenite white, and Bainite Brown)

samples showed tensile elongation of more than 22%, with high tensile strengths of above 780 MPa.

Tensile stress-strain curves of all the samples heated isothermally at 460 °C for different IBT times are given in Fig. 6. Two types of stress-strain curves were obtained illustrating the continuous and discontinuous yielding behavior, respectively. Samples A (t_{IBT} = 10 s) and B (t_{IBT} = 20 s), show a continuous yielding behavior similar to that of high strength ferrite-martensite dual phase steel. Tensile strengths ranging from 870 to 883 MPa with elongation around 18.00-22.44% were obtained in those samples. Continuous yielding behavior is considered to be caused by the smaller volume fractions of retained austenite and a large amount of martensite formed during final cooling. Thus, the dual-phase strengthening effect is considered to be more dominant than the TRIP effect (Ref 12) in samples A (t_{IBT} = 10 s) and B (t_{IBT} = 20 s). On the other hand, a discontinuous yielding behavior was observed in samples C (t_{IBT} = 30 s) and D (t_{IBT} = 60 s). Sakuma reported that the yield point elongation in TRIP steel is due to the low density of dislocations in ferrite grains (Ref 13).

Figure 7 shows changes of yield strength (YS), tensile strength (TS), elongation (EL), and the strength-ductility balance (TS × EL) for different IBT times. Yield strength increased largely from the 356 to 448 MPa level due to the formation of bainite (Ref 11). Tensile strength decreased with

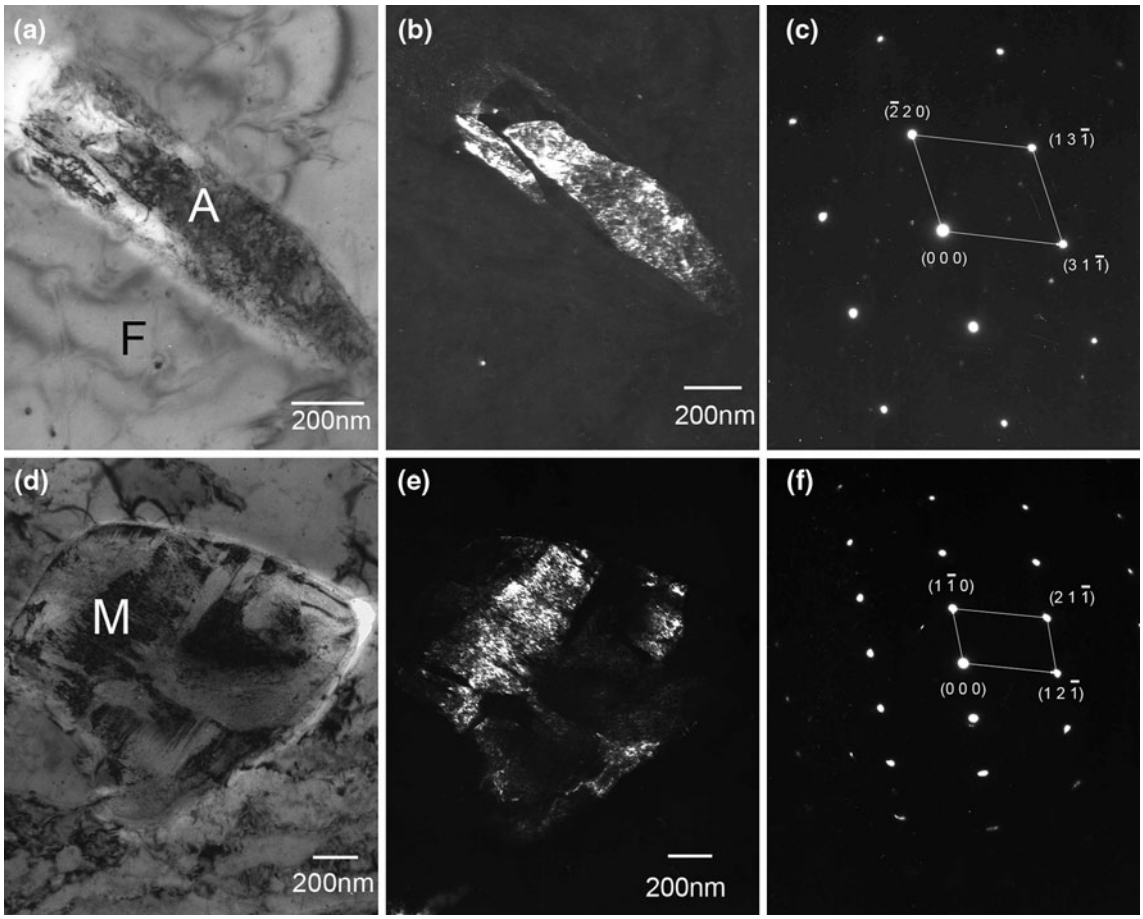

Fig. 4 TEM micrographs of the sample C: (a-c) bright field, dark field, and selected area diffraction of Austenite, respectively; (d-f) bright field, dark field, and selected area diffraction of Martensite, respectively (A: austenite; F: ferrite; M: martensite)

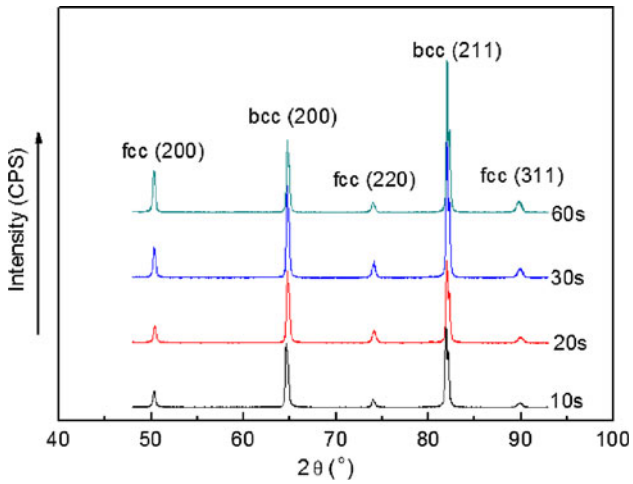

Fig. 5 Effect of IBT time on the profiles of XRD

an increase of the IBT time, especially obvious on the sample D (t_{IBT} = 60 s). The elongations were larger than 22% except the sample A (t_{IBT} = 10 s), and their maximum values reached 28%. A composition of the four specimens in terms of overall tensile properties showed that the mechanical properties were decided by the IBT time. Because the TRIP-aided steels combine high strength with high elongation, the strength-ductility balance (TS × EL) is often used to characterize their mechanical properties. Sample D (t_{IBT} = 60 s) had the best properties, and its strength-ductility balance was greater than 22000 MPa%.

Table 3 Volume fraction and carbon content of retained austenite

Sample code	Retained austenite content, %	2θ of fcc(220), °	Retained austenite carbon content, %
A	9.40	74.089	1.06
B	12.79	74.058	1.09
C	13.82	74.041	1.10
D	15.42	73.979	1.16

Table 4 Tensile test results of the investigated steel

Sample code	YS, MPa	TS, MPa	EL, %	YS/TS	TS × EL, MPa%
A	356	883	18.00	0.40	15894.00
B	365	870	22.44	0.42	19522.80
C	406	841	24.00	0.48	20184.00
D	448	785	28.40	0.57	22294.00

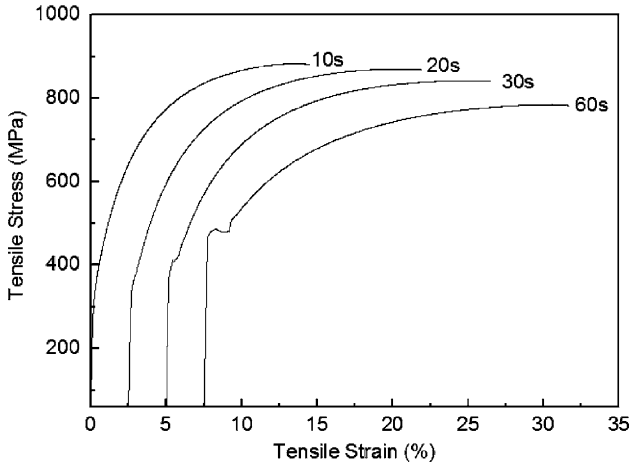

Fig. 6 Tensile stress-strain curves of samples with different IBT time

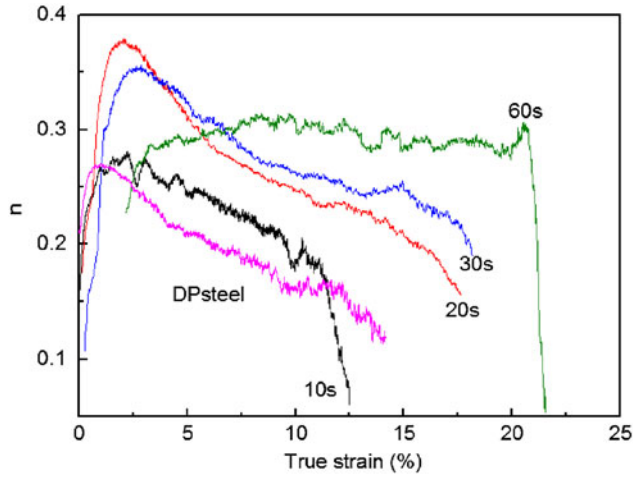

Fig. 8 Variation of the incremental work-hardening exponent (n) with true strain of samples and DP steel

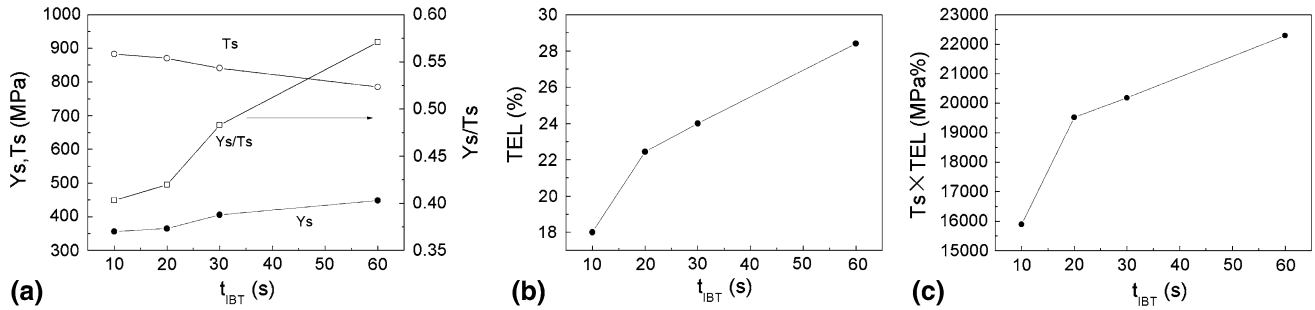

Fig. 7 Variation of (a) strength (Ys;Ts, and Ys/Ts), (b) elongation, and (c) the strength-ductility balance with various IBT time

The strain hardening behavior of the four samples was studied. The instantaneous strain hardening coefficient, n, was calculated by means of the Eq 2 (Ref 5).

$$n = \frac{d(\ln \sigma)}{d(\ln \varepsilon)} \qquad \text{(Eq 2)}$$

where σ is the true stress, and ε is the true strain.

Figure 8 shows the change in the instantaneous n value during tensile testing. It can be seen that the n value of the samples for the IBT time from 10 s (sample code A) to 30 s (sample code C) increased greatly to the maximum value at the beginning of straining, and then decreased continuously from a maximum value ranging from 0.27 to 0.37. The highest maximum value corresponds to the sharpest drop with further straining. However, the samples with a longer IBT time exhibit higher n value during further straining. For reference, the n value of typical DP steel is shown in Fig. 8. The DP steel shows high n value in the low strain region, and monotonous decreases in n value with the increase of strain. The n value characteristics of the samples for the IBT time from 10 s (sample code A) to 30 s (sample code C) are similar to those of the DP steel. In fact, dual-phase steels usually contain retained austenite; however, their stability is very low, and they get easily transformed to martensite (Ref 14). In contrast to the samples A, B, and C, the n value of the samples D (t_{IBT} = 60 s) shows a different behavior as shown in Fig. 8. In that way, n value is low in the beginning but increases with strain, and is kept high until fracture takes place.

The longer the bainite transformation time, the more the volume fraction of the retained austenite remains. In other words, the retained austenite obtained after short time bainite transformation is plastically unstable. From Fig. 8, it is possible to relate the work-hardening behavior to the stability of retained austenite against deformation. Work hardening occurs when the retained austenite transforms to martensite. As a result, n value becomes high. Since the plastically unstable retained austenite transforms in the early stage of deformation, it leads to the high n value only at this deformation stage. Therefore, this kind of austenite is not thought to improve the strength-ductility balance.

4. Conclusion

1. The microstructure of the hot-dip galvanized TRIP steel samples consists of ferrite, bainite, retained austenite, and martensite. Martensitic transformation is considered to occur from the unstable retained austenite with low carbon content for short IBT time.
2. The elongation and the amount of retained austenite increased with the increments of IBT time. For an IBT time of 10 s, the volume fraction of the retained austenite

and the percent elongation were 9.40 and 18%, respectively, and for an IBT time of 60 s, the volume fraction of the retained austenite and percent elongation were 15.42 and 28.4%, respectively.

3. The *n* value characteristics of the samples are similar to those of DP steel for the IBT time from 10 to 30 s. On the contrary, the *n* value of the specimen bainite transformed for 60 s shows a notable feature of typical TRIP steel.

Acknowledgment

This investigation was supported by the National Natural Science Foundation of China (No. 50804005).

References

1. B.C. De Cooman, Structure-Properties Relationship in TRIP Steels Containing Carbide-Free Bainite, *Curr. Opin. Solid State Mater. Sci.*, 2004, **8**(3–4), p 285–303
2. B. Mintz, Hot Dip Galvanising of Transformation Induced Plasticity and Other Intercritically Annealed Steels, *Int. Mater. Rev.*, 2001, **46**(4), p 169–197
3. V.F. Zackay, E.R. Parker, D. Fahr, and R.A. Busch, The Enhancement of Ductility in High-Strength Steels, *ASM Trans. Quart.*, 1967, **60**(2), p 252–259
4. O. Matsumura, Y. Sakuma, and H. Takechi, Trip and Its Kinetic Aspects in Austempered 0.4C-1.5Si-0.8Mn Steel, *Scripta Metall.*, 1987, **21**(10), p 1301–1306
5. P.J. Jacques, E. Girault, A. Mertens, B. Verlinden, J. van Humbeeck, and F. Delannay, The Developments of Cold-rolled TRIP-Assisted Multiphase Steels. Al-Alloyed TRIP-Assisted Multiphase Steels, *ISIJ Int.*, 2001, **41**(9), p 1068–1074
6. H.T. Jiang, H.B. Wu, D. Tang, and Q. Liu, Influence of Isothermal Bainitic Processing on the Mechanical Properties and Microstructure Characterization of TRIP Steel, *J. Univ. Sci. Technol. Beijing Miner. Metall., Mater.*, 2008, **15**(5), p 574–579
7. E.M. Bellhousea and J.R. McDermid, Analysis of the Fe-Zn Interface of Galvanized High Al-Low Si TRIP Steels, *Mater. Sci. Eng. A*, 2008, **491**(1–2), p 39–46
8. E.M. Bellhouse, A.I.M. Mertens, and J.R. McDermid, Development of the Surface Structure of TRIP Steels Prior to Hot-Dip Galvanizing, *Mater. Sci. Eng. A*, 2007, **463**(1–2), p 147–156
9. L. Li, B.C. De Cooman, R.D. Liu, J. Vleugels, M. Zhang, and W. Shi, Design of TRIP Steel with High Welding and Galvanizing Performance in Light of Thermodynamics and Kinetics, *J. Iron Steel Res. Int.*, 2007, **14**(6), p 37–41
10. A.K. De, J.G. Speer, and D.K. Matlock, Color Tint-Etching for Multiphase Steels, *Adv. Mater. Process.*, 2003, **161**(2), p 27–30
11. K. Sugimotom, M. Misu, M. Kobayashi, and H. Shirasawa, Effects of Second Phase Morphology on Retained Austenite Morphology and Tensile Properties in a TRIP-Aided Dual-Phase Steel Sheet, *ISIJ Int.*, 1993, **33**(7), p P775–P782
12. S.J. Kim, C.G. Lee, T.H. Lee, and C.S. Oh, Effect of Cu, Cr and Ni on Mechanical Properties of 0.15 wt.% C TRIP-Aided Cold Rolled Steels, *Scripta Mater.*, 2003, **48**(5), p 539–544
13. Y. Sakuma, D.K. Matlock, and G. Krauss, Intercritically Annealed and Isothermally Transformed 0.15 Pct C Steels Containing 1.2 Pct Si-1.5 Pct Mn and 4 Pct Ni: Part I. Transformation, Microstructure, and Room-Temperature Mechanical Properties, *Metall. Mater. Trans. A*, 1992, **23**(A), p 1221–1232
14. M.H. Saleh and R. Priestner, Retained Austenite in Dual-Phase Silicon Steels and Its Effect on Mechanical Properties, *J. Mater. Process. Technol.*, 2001, **113**(1–3), p 587–593